J. Biochem. 130, 789–797 (2001)

Adrenodoxin–Cytochrome P450scc Interaction as Revealed by EPR Spectroscopy: Comparison with the Putidaredoxin–Cytochrome P450cam System[1]

Kohji Takeuchi,* Motonari Tsubaki,*,†,2 Junya Futagawa,‡ Futoshi Masuya,‡ and Hiroshi Hori‡

*Department of Life Science, Faculty of Science, Himeji Institute of Technology, Kamigoori-cho, Akou-gun, Hyogo 678-1297; †Institute for Protein Research, Osaka University, Suita, Osaka 565-0871; and ‡Division of Biophysical Engineering, Graduate School of Engineering Science, Osaka University, Toyonaka, Osaka 560-8531

Received August 24, 2001; accepted September 28, 2001

The cholesterol side-chain cleavage reaction catalyzed by cytochrome P450scc comprises three consecutive monooxygenase reactions (22R-hydroxylation, 20S-hydroxylation, and C_{20}-C_{22} bond scission) that produces pregnenolone. The electron equivalents necessary for the oxygen activation are supplied from a 2Fe-2S type ferredoxin, adrenodoxin. We found that 1:1 stoichiometric binding of oxidized adrenodoxin to oxidized cytochrome P450scc complexed with cholesterol or 25-hydroxycholesterol caused shifts of the high-spin EPR signals of the heme moiety at 5 K. Such shifts were not observed for the low-spin EPR signals. Ligation of CO or NO to the reduced heme of cytochrome P450scc complexed with reduced adrenodoxin and various steroid substrates did not cause any change in the axial EPR spectrum of the reduced iron-sulfur center at 77 K. These results are in remarkable contrast to those obtained for the cytochrome P450cam–*d*-camphor–putidaredoxin ternary complex, suggesting that the mode of cross talk between adrenodoxin and cytochrome P450scc is very different from that in the *Pseudomonas* system. The difference may be primarily due to the location of the charged amino acid residues of the ferredoxins important for the interaction with the partner cytochrome P450.

Key words: adrenodoxin, cytochrome P450cam, cytochrome P450scc, EPR, putidaredoxin.

The cholesterol side-chain cleavage reaction catalyzed by cytochrome P450scc (P450scc; CYP11A1) comprises three consecutive monooxygenase reactions; *i.e.*, hydroxylation at the 22R-position, hydroxylation at the 20S-position, and C_{20}-C_{22} bond scission. Three molecules of dioxygen and six electron equivalents are required to accomplish the side-chain cleavage reaction. The electron equivalents are supplied from a 2Fe-2S type iron-sulfur protein, adrenodoxin (Adx), which can accommodate a single electron equivalent supplied from a flavin-containing NADPH-adrenodoxin reductase (AR). Each monooxygenase cycle consists of the following five steps. (a) Substrate binding to P450scc in the oxidized state, (b) first electron transfer from reduced Adx (Adx^{red}) to the ferric heme, (c) dioxygen binding to the ferrous heme iron, (d) second electron transfer from Adx^{red} to the dioxygen-bound ferrous heme iron, and (e) dioxygen activation followed by hydroxylation of the substrate (see reviews such as Ref. *1*).

Since Adx is a small (MW ~ 14,000) and highly acidic protein, the nature of the interaction between P450scc and Adx was believed to be electrostatic (*2*). Coghlan and Vickery found that the Asp residues at positions 76 and 79 of human Adx are important for binding to P450scc based on a site-directed mutagenesis study (*3*), suggesting that the Adx-binding site of P450scc involves basic amino acids. Based on specific chemical modification studies (*4, 5*), the putative Adx-binding site was proposed to exist at the surface of P450scc proximal to the heme iron, which is coordinated with a cysteinyl thiolate ligand (*4*). Indeed, the identified Adx-binding sequence in the K-helix contains Lys residues at positions 377 and 381, and an Arg residue at position 385, all of which are exclusively conserved among the mitochondrial cytochrome P450 subfamily including cytochromes P450scc (*6*), P45011β (*7*), P450c27 (*8*), $P450D_3$-1α (*9*), and $P450D_3$-24 (*10*). This proposal was later confirmed by site-directed mutagenesis studies of P450scc (*11*) and P450c27 protein (*12*). The substitution of the conserved Lys residues with neutral or negatively charged residues caused extensive decreases in the interaction with oxidized Adx (Adx^{ox}) and in the enzymatic activity (*11, 12*).

Upon the event of the electron transfer reaction from Adx to P450scc, two types of ternary complex might be formed; *i.e.*, the Adx^{red}-oxidized P450scc-substrate complex and the

[1] This work was supported in part by Grants-in-Aid for Scientific Research on Priority Areas (12050236 to MT) and for Scientific Research (C) (12680659 to MT) from the Ministry of Education, Science, Sports and Culture of Japan.

[2] To whom correspondence should be addressed. Tel: +81-791-58-0189, Fax: +81-791-58-0189, E-mail: tsubaki@sci.himeji-tech.ac.jp

Abbreviations: Adx, adrenodoxin; AR, NADPH-adrenodoxin reductase; P450scc, cytochrome P450scc (CYP11A1); SF, substrate-free; Pdx, putidaredoxin; P450cam, cytochrome P450cam (CYP101).

Adx^{red}-oxygenated P450scc-substrate complex. The second one is of particular interest. We previously showed that the addition of Adx^{red} to reduced P450scc complexed with phenylisocyanide caused a visible spectral change in the heme absorption (*13*). Since this spectral change showed clear saturation with a 1:1 stoichiometry, it was suggested that the binding of Adx^{red} on the proximal surface of the P450scc molecule caused a conformational change around the ferrous heme moiety (*13*). Similar spectral perturbation at the heme moiety upon Adx^{red}-binding was observed for the ferrous heme-NO complex (*14*) and the ferrous heme-CO complex (*15*) of P-450scc. Therefore, perturbation of the electronic structure at the heme moiety upon the binding of Adx^{red} might be a common phenomenon, and may be related to the electron transfer and the following oxygen activation event.

Very recently, it was shown that the binding of ligands such as CO, NO, and O_2 to the reduced heme iron of the analogous ternary complex [reduced putidaredoxin (Pdx^{red})–reduced cytochrome P450cam–*d*-camphor complex] in *Pseudomonas putida* caused a change in the EPR spectra of Pdx^{red} (*16*). This result was interpreted as showing that a change in the active site of cytochrome P450cam (P450cam) upon ligand binding was transmitted to Pdx^{red} within the ternary complex and produced a conformational change of the 2Fe-2S active center (*16*). Thus, analyses of the interaction between P450 and its electron donor, iron-sulfur protein, are increasingly important for clarifying the mechanism of the oxygen activation at the heme center in detail.

In the present study, the interaction between Adx and P450scc was examined by EPR spectroscopy in both the reduced and oxidized states to reveal the mechanism of the transmission of the conformational change in the ternary complex. The present results suggest that the mode of cross talk between Adx and P450scc is very different from that in the *Pseudomonas* system.

EXPERIMENTAL PROCEDURES

Materials—P450scc(SF) and Adx were purified from bovine adrenocortical mitochondria to homogeneity as previously described (*17, 18*). P450scc(SF) and P450scc-substrate complexes in 20 mM potassium phosphate buffer (pH 7.4) containing 20% (v/v) glycerol and 0.1 mM EDTA (buffer A) were prepared as previously described (*19*), and were concentrated to about 0.5–0.6 mM. For use, the samples were diluted appropriately with buffer A. Adx in buffer A was added in excess to the P450scc-substrate complex in the ratio of 1:1.2 when the heme moiety was examined by EPR spectroscopy. On the other hand, excess P450scc was added (in the ratio of 1:1.2) when the iron-sulfur cluster moiety was examined. For a titration experiment with Adx^{ox}, P450scc–25-hydroxycholesterol complex in the oxidized state (at 169.7 μM) was mixed with various concentrations (from 0 to 316.2 μM) of Adx^{ox} in buffer A. To examine the effect of glycerol, Adx, the P450scc–25-hydroxycholestrol complex, and the ternary complex were prepared in 20 mM potassium phosphate buffer (pH 7.4) and 0.1 mM EDTA (buffer B), and then concentrated and diluted appropriately with buffer B.

P450cam and Pdx expressed in *Escherichia coli* were purified to homogeneity as described previously (*16, 20*), and then concentrated and diluted appropriately with either buffer A or buffer B. The expression vectors for the P450cam and Pdx genes were kindly supplied by Dr. Hideo Shimada (Keio University).

Measurements of EPR Spectra—A 150 μl solution containing either Adx or Adx *plus* P450scc in buffer A or buffer B was transferred to a screw-capped EPR tube. The proteins were reduced with sodium dithionite as previously described (*16*). When necessary, CO or NO gas was anaerobically introduced to the EPR tube containing Adx^{red} and reduced P450scc. For the Pdx-P450cam system, samples were reduced in a similar manner to as previously described (*16*).

EPR measurements were carried out at an X-band (9.35 GHz) microwave frequency with a Varian E-12 EPR spectrometer (San Fernando, CA) with following instrumental parameters: microwave power, 5 mW; modulation frequency, 100 kHz; and modulation amplitude, 0.5 mT. An immersion Dewar flask was used for the measurements at liquid nitrogen temperature (77 K); whereas an Oxford flow cryostat (ESR-900) was used for measurements at 5 and 15 K. The microwave frequency was calibrated with a microwave frequency counter (Takeda Riken, model TR5212). The magnetic field strength was determined as the nuclear magnetic resonance of protons in water. The accuracy of the *g*-values was approximately ± 0.001.

MALDI-TOF Mass Spectrometry—Mass spectrometric analyses of P450scc and Adx were carried out on a Voyager RP mass spectrometer (Perseptive Biosystems, Farmingham, MA, USA) using an accelerating voltage of 20 kV, as described previously (*21*).

RESULTS

EPR Signals of the Ferric Heme of P450scc—The EPR spectrum of the ferric heme of P450scc is strongly dependent on the structure of the bound substrate (*19*). In the substrate-free (SF) state, the heme iron was in the pure

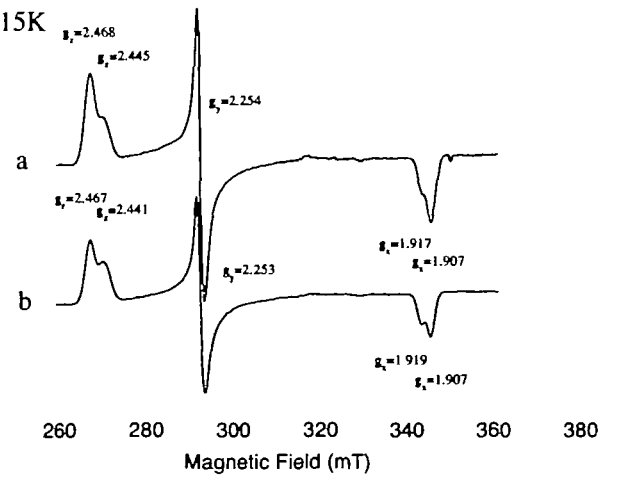

Fig. 1. **EPR spectra of ferric low-spin signals of the P450scc–22*R*-hydroxycholesterol complex in the absence and presence of Adx^{ox}.** EPR spectra of 148 μM P450scc were obtained at 15K in 20 mM potassium phosphate, pH 7.4, containing 20% glycerol and 0.1 mM EDTA in the absence of Adx (a) and in the presence of 178 μM Adx^{ox} (b).

low-spin state. Binding of 22*R*-hydroxycholesterol (or 22*S*-hydroxycholesterol, 20*S*-hydroxycholesterol, or 22-ketocholesterol) maintained the spin equilibrium almost completely in the low-spin state at both room and low (15 K) temperatures (*19*). On the other hand, binding of cholesterol or 25-hydroxycholesterol caused a shift of the spin equilibrium almost completely to the high-spin state at room temperature. Nevertheless, in the low temperature (15 K) EPR spectra, these complexes showed low-spin signals of significant intensity, as previously reported (*19, 22*). Complex formation of these oxidized P450scc with Adx^{ox} did not cause any appreciable change in any of these low-spin EPR signals. A representative example is shown in Fig. 1, in which oxidized P450scc formed a complex with 22*R*-hydroxycholesterol in the presence (Fig. 1b) or absence (Fig. 1a) of Adx^{ox} (1:1.2 ratio). Three *g*-values (g_z = 2.468, g_y = 2.254, and g_x = 1.907) of the low-spin species did not show any appreciable change upon the Adx^{ox}-binding, although a relative population of the two low-spin species became slightly perturbed (Fig. 1).

The high-spin EPR signals derived from the ferric heme of P450scc were examined for the cholesterol- and 25-hydroxycholesterol-complexes. The oxidized P450scc-cholesterol complex without Adx^{ox} showed both high-spin (g = 8.08, g = 3.56, and g = 1.675) and low-spin (g_z = 2.425, g_y = 2.248, and g_x = 1.910) signals at 15 K (Fig. 2, A-a). The addition of Adx^{ox} in a slight excess amount (in the ratio of 1:1.2) did not have any effect on the low-spin signal, as found for the low-spin species of the P450scc-22*R*-hydroxycholesterol complex. However, the high-spin EPR signal showed a drastic change upon the addition of Adx^{ox}. All three components showed significant shifts to g = 8.12, g = 3.49, and g = 1.657, respectively (Fig. 2, A-b). This indicates that the *g*-anisotropy in the heme-plane increased significantly. For clarification, the g8 component of the high-spin signal was examined further at 5 K. In the absence of Adx, the g8 signal showed a peak at g = 8.08; whereas in the presence of Adx^{ox}, it shifted to g = 8.12 (Fig. 2B). In the case of the P450scc–25-hydroxycholesterol complex, very similar spectral changes occurred (spectra not shown). The EPR spectrum in the absence of Adx showed both high-spin (g = 8.08, g = 3.57, and g = 1.683) and low-spin (g_z = 2.418, g_y = 2.249, and g_x = 1.912) signals at 15 K. The addition of Adx^{ox} in a slight excess amount (in the ratio of 1:1.2) did not have any appreciable effect on the low-spin signal. However, the high-spin signal showed a drastic change with significant *g*-value shifts to 8.12, 3.51, and 1.669, respectively.

To clarify the stoichiometry of the Adx-binding to oxidized P450scc, we analyzed the shifts of the high-spin signals (for both the g = 8 and g = 1.65 signals) at 5 K of the P450scc–25-hydroxycholesterol complex in the presence of various concentrations of Adx^{ox}. As shown in Fig. 3, the shift of the g8 high-spin signal from g = 8.08 (without Adx) to g = 8.12 (with Adx^{ox}) was almost completed at around the ratio of 1:1, and there was no further shift upon the addition of excess Adx^{ox}. For the high-spin signal around g = 1.65, a very similar result was obtained. The shift from g = 1.690 (without Adx) to g = 1.675 (with Adx^{ox}) was completed at around the ratio of 1:1, and there was no further shift (spectra not shown). These results suggest that Adx^{ox} forms a complex with oxidized P450scc with a 1:1 stoichiometry.

EPR Signals of the Ferric Heme of P450cam—The EPR

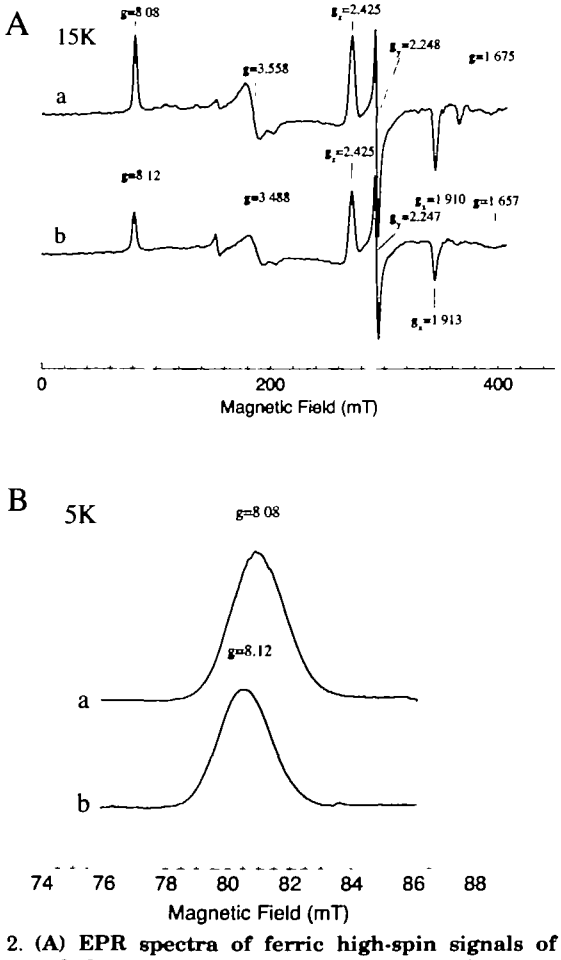

Fig. 2. (A) EPR spectra of ferric high-spin signals of the P450scc-cholesterol complex in the absence and presence of Adx^{ox}. (B) Expanded spectra of ferric g8 high-spin signals of the P450scc-cholesterol complex in the absence and presence of Adx^{ox}. EPR spectra of 170 μM P450scc were obtained at 15 K (A) and 5 K (B) in 20 mM potassium phosphate, pH 7.4, containing 20% glycerol and 0.1 mM EDTA in the absence of Adx (a) and in the presence of 205 μM Adx^{ox} (b).

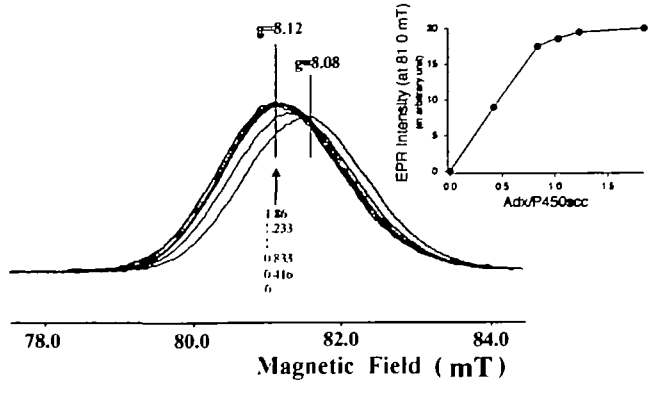

Fig. 3. Effect of Adx^{ox}-binding on the ferric g8 high-spin signal of the P450scc–25-hydroxycholesterol complex. The numbers below the arrow indicate the molar ratios of Adx^{ox} relative to P450scc. The inset shows a plot of the EPR intensity at the magnetic field of 81.0 mT in the spectra. The conditions for the EPR measurements were the same as in Fig. 2, except for the P450scc concentration (178.2 μM).

spectrum of the oxidized P450cam–*d*-camphor complex at 5 K showed both high- (g = 7.90, 3.97, 1.772) and low-spin (g_z = 2.415, g_y = 2.241, g_x = 1.977) signals (Fig. 4, A-a). The addition of a slight excess amount (1:1.2) of Pdx^{ox} had significant effects on the EPR spectrum. First, the relative population of the low- and high-spin species changed significantly, favoring the low-spin state, as previously reported (*23*). Second, the g-values for both the low- and high-spin signals showed significant changes, leading to increases in the g-anisotropy. The g-values for the low-spin species were now 2.435, 2.234, and 1.969, respectively, whereas the g-values for the high-spin species were g = 8.02 and g = 3.82. For clarification, the high-spin g8 signal was further examined at 5 K. It showed a clear shift from g = 7.87 (without Pdx) to g = 8.02 (with Pdx^{ox}) at 5 K (Fig. 4B, a and b). Spectral changes for the low-spin species upon Pdx^{ox}-binding were reported previously by Lipscomb (*23*), but the shift of the high-spin signals of P450cam is reported for the first time.

EPR Signal of the Adx Iron-Sulfur Center—The EPR spectrum of Adx^{red} alone showed a characteristic axial signal with $g_{//}$ = 2.024 and $g_{\perp}$ = 1.937 originating from the iron-sulfur center at 77 K (Fig. 5, a). Complex formation with reduced P450scc(SF) did not have any appreciable influence on the EPR signal of the iron-sulfur center (spectrum not shown). Ternary complex formation upon preaddition of various substrates (including cholesterol, 20*S*-hydroxycholesterol, 22*R*-hydroxycholesterol, 22*S*-hydroxycholesterol, 25-hydroxycholesterol, and 22-ketocholesterol) to P450scc also did not significantly affect the EPR signal of the iron-sulfur center. Only the data for the reduced P450scc–cholesterol–Adx^{red} ternary complex are shown (Fig. 5, b). The addition of CO (Fig. 5, c) or NO (spectrum not shown) to the ternary complex did not cause any appreciable changes either. Careful analyses involving difference spectroscopy (reduced ternary complex *minus* Adx^{red} alone, and CO-reduced ternary complex *minus* reduced ternary complex) confirmed that there were negligible shifts for both the $g_{//}$ = 2.024 and $g_{\perp}$ = 1.937 signals for the ternary complexes with cholesterol, 22*R*-hydroxycholesterol, 22*S*-hydroxycholesterol, and 22-ketocholesterol (spectra not shown).

Ternary complex formation with the reduced P450scc–20*S*-hydroxycholesterol complex caused a spectral change in the difference spectrum of Adx^{red}, giving a trough at 348.1 mT (spectrum not shown). Binding of CO to the ferrous heme iron of P450scc–20*S*-hydroxycholesterol in the ternary complex also caused a trough at 348.1 mT in the difference spectrum. These spectral changes were found, however, to be due to the residual g_x-component of the low-spin species from the oxidized P450scc–20*S*-hydroxycholesterol complex. Since this steroid complex is very resistant to reduction with sodium dithionite, this type of negative peak at 348.1 mT persisted after the usual incubation on ice. Prolonged incubation of the ternary complex (with or without CO) caused the complete loss of this negative peak.

Effects of Glycerol—The effects of depletion of glycerol from the buffer on the EPR signals of Adx^{red} were examined. No spectral change was observed between the EPR spectra for Adx^{red} alone, the reduced P450scc–25-hydroxycholesterol–Adx^{red} ternary complex, and the CO-reduced

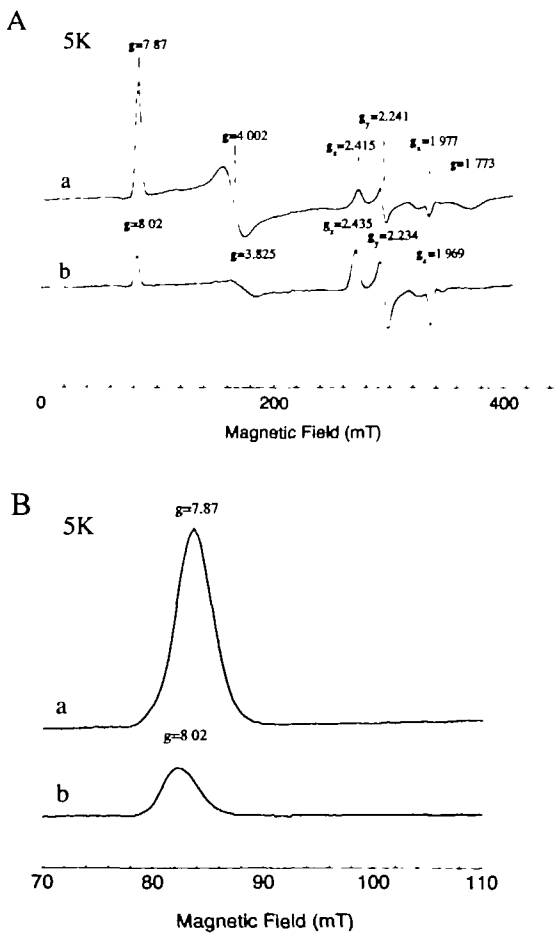

Fig. 4. **(A) EPR spectra of ferric high- and low-spin signals of the P450cam–*d*-camphor complex in the absence and presence of Pdx^{ox}. (B) Expanded spectra of ferric g8 high-spin signals of the P450cam–*d*-camphor complex in the absence and presence of Pdx^{ox}.** EPR spectra of 170 μM P450cam were obtained at 5 K in 20 mM potassium phosphate, pH 7.4, containing 20% glycerol and 0.1 mM EDTA in the absence of Pdx (a) and in the presence of 205 μM Pdx^{ox} (b).

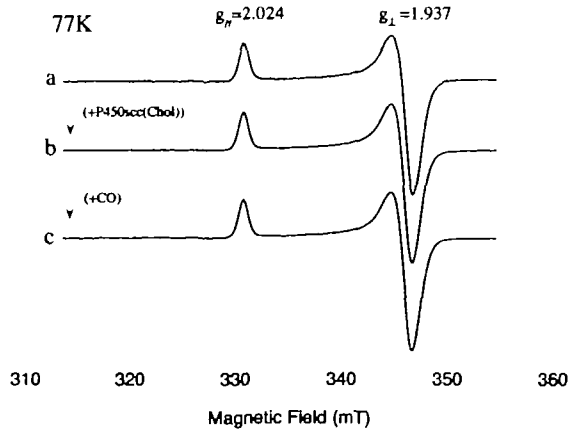

Fig. 5. **EPR spectra of Adx^{red} in the absence and presence of the P450scc-cholesterol complex and CO.** EPR spectra of 148 μM Adx^{red} were obtained at 77 K in 20 mM potassium phosphate, pH 7.4, containing 20% glycerol and 0.1 mM EDTA in its free state (a), in the presence of 178 μM of the ferrous P450scc-cholesterol complex without CO (b) and with excess CO (c).

ternary complex, all prepared in buffer B (spectra not shown). The spectra were almost identical with those of the corresponding species prepared in buffer A. Therefore, we infer that the absence of the spectral change of the 2Fe-2S center of Adx^{red} in the ternary complexes and in the CO-reduced ternary complexes is not due to the presence of glycerol in the buffer used, but due to its intrinsic nature.

The effects of the addition of glycerol on the EPR signal from Pdx^{red} were also examined. In the absence of glycerol (*i.e.*, in buffer B), a trough of the $g_{\perp}$ signal was observed at 346 mT, as previously reported (*16*). In the presence of 20% (v/v) glycerol (*i.e.*, in buffer A), the trough showed a shift to 347 mT (spectra not shown). The ternary complex formation with the reduced P450cam–*d*-camphor complex in buffer A did not cause any further changes in the EPR signal from Pdx^{red} (spectra not shown). However, the addition of CO to the reduced ternary complex in buffer A caused significant sharpening of the trough at 348 mT (spectra not shown), resulting in very similar spectra to those of the CO-reduced P450cam–*d*-camphor–Pdx^{red} ternary complex in the absence of glycerol (*16*). Thus, even in the presence of 20% (v/v) glycerol, ligand binding to the reduced heme center of P450cam caused a change in the EPR signal from Pdx^{red} within the same ternary complex. The details of the effect of glycerol on the EPR signals from Pdx^{red} will be published elsewhere.

MALDI-TOF Mass Spectrometry—Since Adx and P450scc used in the present study were prepared from bovine adrenal cortex, rather than being cloned and expressed proteins, the heterogeneity of the samples was examined by MALDI-TOF mass spectrometry. It has been reported that proteolysis of Adx during purification occurs due to contamination of adrenal cortex preparations by small amounts of adrenal medulla containing trypsin-like and carboxypeptidase activities (*24*). The mass spectra of P450scc showed a clear $[M+H^+]$ peak at 56,366.0 (m/z) (spectra not shown). This value is very close to the theoretical value (56,378.3) of the mature form (residues 1–481) based on the deduced amino acid sequence (*6*). The mass spectra of Adx showed a multiple $[M+H^+]$ peak in the region of 12,400 to 14,050 (m/z) (spectra not shown). The peaks with the highest and lowest m/z values (14,041.0 and 12,400.0) correspond to the mature Adx form (residues 1–128; theoretical molecular weight, 14,042.8) and a truncated form (residues 1–113; theoretical molecular weight, 12,392.9), respectively, based on the deduced amino acid sequence (*25*). A major peak appeared at 12,626.5 (m/z), which corresponds to a truncated form (residues 1–115) with a theoretical molecular weight of 12,620.2.

DISCUSSION

In the present study we showed that the conformational change occurring upon binding of Adx^{ox} at the protein surface of P450scc could be transmitted to the ferric heme center. The titration experiment with Adx^{ox} showed a clear shift in the *g*-value of the high-spin EPR signals from the P450scc–25-hydroxycholesterol complex with a 1:1 stoichiometry (Fig. 3), indicating the binding of Adx^{ox} to a specific site on the surface of the P450scc molecule. It should be noted that such shifts in the *g*-value were observed only for the high-spin species (Fig. 2). Even if the same substrate molecule (*i.e.*, 25-hydroxycholesterol or cholesterol) was bound at the substrate-binding site, the low-spin signals did not show any shift in the *g*-value upon the addition of Adx^{ox}. Consistent with this observation, there was no shift in the low spin signals upon Adx^{ox}-binding to the P450scc–22*R*-hydroxycholesterol complex (Fig. 1) (or the 22*S*-hydroxycholesterol, 20*S*-hydroxycholesterol, and 22-ketocholesterol-complexes), in which the high-spin EPR species were almost negligible.

One may argue that Adx^{ox} does not form a tight complex with oxidized P450scc in the low-spin state and, therefore, there might be no effect of the Adx^{ox}-binding on the low-spin signals. However, we previously performed titration of oxidized P450scc in the substrate-free state (fully low-spin state) with Adx^{ox} and found an apparent dissociation constant (K_s) of 0.38 μM based on the spectral change at the Soret band (*4*). This value is comparable to those for Adx^{ox}-binding to the P450scc-cholesterol complex [K_s = 0.8 μM (*3*), and K_s = 0.23 μM (*11*)], indicating high-affinity binding. For the interaction of Adx^{red} with reduced P450scc in the low-spin state, there is ample evidence of the formation of the complex, such as for the CO-reduced (*15, 26*), NO-reduced (*14*), and phenylisocyanide-reduced (*13*) states. Therefore, it is reasonable to assume that P450scc forms a complex with Adx irrespective of the oxidation state or spin state at the sub-micromolar concentration.

The higher sensitivity of the high-spin species to the conformational change at the protein surface may be related to the local conformation around the heme center. The absence of the heme axial ligand *trans* to the proximal thiolate ligand may reduce the conformational rigidity around the heme moiety, leading to the increased flexibility as to the conformational change of the protein. On the other hand, the low-spin heme center, where an H_2O or hydroxide ion is expected to be coordinated to form a relatively rigid hydrogen bond network with surrounding amino acid residues and a substrate molecule, could sustain the conformational change at the protein surface caused by Adx-binding. The presence of the substrate molecule must be very important for the rigidity of the low-spin species of P450scc, since clear spectroscopic evidence of Adx-binding was obtained exclusively in the absence of the steroid substrate (*13, 14*).

Comparison with the P450cam-Pdx system gave us very interesting results. The apparent dissociation constant of the Pdx^{ox}-binding to the oxidized P450cam–*d*-camphor complex [K_s = 10–30 μM (*27*), and K_s = 16.8 μM (*28*)] suggests a much weaker interaction than in the oxidized P450scc-Adx^{ox} system. However, the observed shifts of the *g*-values for the high-spin EPR signals upon binding of Pdx^{ox} (Fig. 4A) were even larger than those for the P450scc-cholesterol (Fig. 2A) and P450scc–25-hydroxycholesterol complexes. Further, the Pdx^{ox}-binding caused changes in both the spin equilibrium and the *g*-values of the low-spin signals as well (Fig. 4A). The shift in the spin equilibrium favoring the low-spin state was very significant, as reported previously by Lipscomb (*23*). (A much smaller spin equilibrium shift favoring the low-spin state was observed upon binding of Adx^{ox} to the P450scc-cholesterol complex, as shown in Fig. 2A.) He also reported the changes in the low-spin signal upon the Pdx^{ox}-binding (*23*). Consistent with this observation, there is much spectroscopic evidence of the formation of the P450cam-Pdx complex in the low-spin states [for CN-oxidized (*29*) and CO-reduced (*30*) states].

Thus, it may be concluded that the effect of the ferredoxin-binding on the heme moiety is much more extensive for the P450cam–*d*-camphor complex than the corresponding species of P450scc, suggesting the increased flexibility of P450cam. The large difference in the downshifts of the bound C-O stretching vibration upon binding of the reduced ferredoxin partner [8.0 cm^{-1} for the P450cam–*d*-camphor–CO complex (*30*), and 0.1–3.3 cm^{-1} for various P450scc-substrate-CO complexes (*15*)] is also consistent with this view.

On the other hand, no spectral change occurred in the EPR spectra for the reduced iron-sulfur moiety of Adx upon the addition of P450scc alone or P450scc *plus* heme ligand, irrespective of the nature of the bound steroid substrate (Fig. 5). This result is also in remarkable contrast with those for the *P. putida* system. Shimada *et al.* showed that the complex formation with reduced P450cam–*d*-camphor alone could induce the EPR spectral change in the $g_{\perp}$ region of the iron-sulfur center of Pdx^{red} (*16*). A further structural change occurred at the iron-sulfur center, giving a very broad $g_{\perp}$ signal upon the binding of CO (NO, or O_2) to the ferrous heme of P450cam (*16*). It was proposed, therefore, that, in the *P. putida* system, a change in the P450cam active site caused by the ligand-binding is transmitted to Pdx^{red} within the ternary complex and then produces a conformational change of the 2Fe-2S active center (*16*). In the present study, we confirmed that such a conformational change of the 2Fe-2S center of Pdx^{red} within the ternary complex could occur even in the presence of 20% (v/v) glycerol.

The apparent discrepancy between the affinities of ferredoxin-binding and the effects of the complex formation on the respective metal center (the heme center and the iron-sulfur center) suggests that there might be a distinct difference in the mode of interaction between the P450scc-Adx complex and the P450cam-Pdx complex, in addition to the difference in the molecular flexibility.

The structure of Pdx^{ox} was solved by NMR spectroscopy (*31, 32*). On the other hand, the X-ray structures of both truncated (residues 4–108) and full-length (residues 2–128) forms of bovine Adx^{ox} were determined and were the same as each other except for a limited number of side-chain orientations (*33, 34*).

Common features to all 2Fe-2S type ferredoxins are the highly negative surface charge and the involvement of acidic residues in the interaction with the redox partners (Fig. 6). The longer C-terminal tail of Adx compared to that of Pdx should be noted (Fig. 6). However, in the X-ray structure, there is no electron density for the C-terminal part of the full-length molecule (residues 112–128) (*34*). Deletion of residues 115–128 (*24*) or 109–128 (*35*) of bovine Adx did not essentially affect the ability of electron transfer to P450scc. These observations suggest that the C-terminal part (residues 112–128) does not have an important role in the structural integrity of Adx or the interaction with P450scc. Our mass spectrometric analyses of Adx suggest that the C-terminal part of Adx is indeed very susceptible to proteolysis, resulting in C-terminal heterogeneity.

Pdx and Adx are both composed of two domains (the "core domain" and the "interaction domain" with a large hairpin structure) and their structures were superimposed taking into account the domains as well as the insertion/deletion (Fig. 7) (*33*). The iron-sulfur center is located in the "core domain" and is close to the protein surface for both Pdx and Adx (*33*). However, the residues involved in the recognition of the P450 partner showed a somewhat larger difference between Pdx and Adx. The charged residues of Adx important for the interaction with P450scc (*i.e.*, Asp72, Glu73, Asp76, and Asp79) (*3*) are all located within the large hairpin structure, *i.e.*, the "interaction domain" (*33, 34*) (Fig. 7). On the other hand, the charged residues of Pdx important for the interaction with P450cam (*i.e.*, Asp34, Asp38, and Trp106 carboxylate) (*36*) reside within the "core domain" (Fig. 7). Thus, it may be expected that the electronic structure at the reduced iron-sulfur center of Adx could be influenced differently from that of Pdx upon complex formation with the P450 partners. Asp34, Asp38, and Trp106 carboxylate of Pdx are very close to the iron-sulfur center (Fig. 7) and, therefore, the conformational change at the P450cam-Pdx interface may be easily reflected by the electronic structure of the iron-sulfur center. Conversely, the electronic structure of the P450scc heme center could be influenced differently from that of P450cam upon complex formation with the ferredoxin partners.

The heme(Fe)-S(Cys) bond of P450 is intrinsically much stronger than the heme(Fe)-N_{ϵ}(His) bond of usual hemopro-

```
Adx   1  SER SER SER GLU ASP LYS ILE THR VAL HIS PHE ILE ASN ARG ASP GLY GLU THR LEU THR THR LYS GLY LYS ILE GLY  27
Pdx   1                          SER LYS VAL VAL TYR VAL SER HIS ASP GLY THR ARG ARG GLU LEU ASP VAL ALA ASP GLY  20

                                                                                  46                      52
Adx  28  ASP SER LEU LEU ASP VAL VAL VAL GLN ASN ASN LEU ASP ILE ASP GLY PHE GLY ALA CYS GLU GLY THR LEU ALA CYS  52
Pdx  21  VAL SER LEU MET GLN ALA ALA VAL SER ASN GLY ILE TYR --- ASP ILE VAL GLY ASP CYS GLY GLY SER ALA SER CYS  45
                                                              34              38  39                      45

                 55                                                               72  73          76
Adx  53  SER THR CYS HIS LEU ILE PHE GLU GLN HIS ILE PHE GLU LYS LEU GLU ALA ILE THR ASP GLU GLU ASN ASP MET LEU  78
Pdx  46  ALA THR CYS HIS VAL TYR VAL ASN GLU ALA PHE THR ASP LYS VAL PRO ALA ALA ASN GLU ARG GLU ILE GLY MET LEU  72
                 48

         79                                                    92
Adx  79  ASP --- LEU ALA TYR GLY LEU THR ASP ARG SER ARG LEU GLY CYS GLN ILE CYS LEU THR LYS ALA MET ASP ASN MET 103
Pdx  73  GLU CYS VAL THR ALA GLU LEU LYS PRO ASN SER ARG LEU CYS CYS GLN ILE ILE MET THR PRO GLU LEU ASP GLY ILE  97
                                                              86

Adx 104  THR VAL ARG VAL PRO ASP ALA VAL SER ASP ALA ARG GLU SER ILE ASP MET GLY MET ASN SER SER LYS ILE GLU     128
Pdx  98  VAL VAL ASP VAL PRO ASP ARG GLN TRP                                                                   106
                                    106
```

Fig. 6. Comparison of the amino acid sequences of Adx and Pdx.

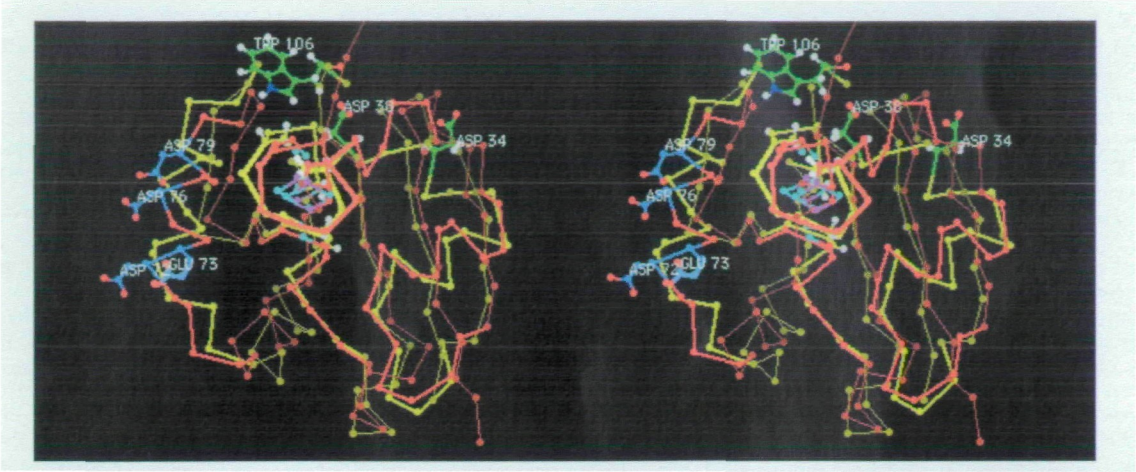

Fig. 7. **Stereo views of the molecular structures of Adx (yellow) and Pdx (red).** The two structures are superimposed based on the least-square fitting algorithm to minimize the distance-squared between pairs of C_α atoms. The figure shows the C_α traces of the two ferredoxins. The [2Fe-2S] clusters are shown as squares in light blue and in purple in the center. Some side chains important for the interaction with P450 partners are shown in blue for Adx (Asp72, Glu73, Asp76, and Asp79) and in green for Pdx (Asp34, Asp38, and Trp104). The atomic coordinates were obtained from the Protein Data Bank ("1AYF" for Adx and "1PUT" for Pdx).

teins (*37*), as indicated by the stronger rhombic distortion of the ferric high-spin EPR signal (*38*). The significant increase in the in-plane *g*-anisotropy of the ferric high-spin EPR signals of P450scc and P450cam upon binding of partner ferredoxins, as observed in the present study (Figs. 2 and 4), indicates a further increase in the heme (Fe^{3+})–S(Cys) bond strength. The results are fully consistent with the resonance Raman observation of Unno *et al.* (*39*). They observed that Pdx^{ox}-binding to the oxidized P450cam–*d*-camphor complex caused an increase in the heme (Fe^{3+})–S(Cys) stretching frequency of the ferric high-spin species by ~3 cm^{-1}. They interpreted this as showing that the negatively charged character of Pdx screens the proximal positive charges on P450cam and promotes sulfur-iron electron donation, leading to the increased Fe-S stretching frequency (*39*). In this context, it may be very informative to examine the effect of Adx^{ox}-binding on the heme (Fe^{3+})–S(Cys) stretching frequency of the ferric high-spin species of P450scc. Adx apparently exhibits stronger binding affinity to the partner P450, as discussed above, although Pdx and Adx bear similar negative charges on the protein surface (having almost the same theoretical pI values of 4.4). We may be able to evaluate the conformational flexibility at the P450scc–Adx interface.

Several models for the physiological electron transfer reactions among P450scc, Adx, and AR have been discussed. These include a shuttle mechanism model in which Adx forms consecutive 1:1 complexes with AR and P450scc (*40*), and models requiring the formation of an organized 1:1:1 ternary complex (*41*) or a 1:2:1 quaternary complex between AR, Adx, and P450scc (*42*). In the present study, we obtained evidence indicating that oxidized Adx forms a 1:1 complex with oxidized P450scc in the presence of a substrate. Previously, we showed that reduced Adx forms a 1:1 complex with reduced P450scc (*13*). Thus, 1:1 complex formation seems to be a general phenomenon for the Adx-P450scc interaction and, therefore, the dimer formation of Adx (*34*) during the electron transfer from AR to P450scc seems unlikely under physiological conditions. On the other hand, a recent X-ray crystallographic study on a covalent 1:1 complex of Adx and AR suggested that the organized 1:1:1 complex is also unlikely (*43*). Further, no steroidogenic hydroxylase activity could be detected in the covalent Adx-P450scc complex/AR test system (*44*). These lines of evidence seem to favor the shuttle mechanism for the physiological electron transfer in the steroidogenic electron transfer system in mitochondria.

We are grateful to Dr. Hideo Shimada, Prof. Yuzuru Ishimura (Keio University), and Prof. Tadao Horiuchi for the gifts of expression vectors P450cam and Pdx.

REFERENCES

1. Jefcoate, C.R. (1986) Cytochrome P-450 enzymes in sterol biosynthesis and metabolism in *Cytochrome P-450 Structure, Mechanism, and Biochemistry* (Ortiz de Montellano, P., ed.) pp. 387–428, Plenum Press, New York and London
2. Lambeth, J.D., Seybert, D.W., and Kamin, H. (1979) Ionic effects on adrenal steroidogenic electron transport. The role of adrenodoxin as an electron shuttle. *J. Biol. Chem.* **254**, 7255–7264
3. Coghlan, V.M. and Vickery, L.E. (1991) Site-specific mutations in human ferredoxin that affect binding to ferredoxin reductase and cytochrome $P450_{scc}$. *J. Biol. Chem.* **266**, 18606–18612
4. Tsubaki, M., Iwamoto, Y., Hiwatashi, A., and Ichikawa, Y. (1989) Inhibition of electron transfer from adrenodoxin to cytochrome $P\text{-}450_{scc}$ by chemical modification with pyridoxal 5′-phosphate: Identification of adrenodoxin-binding site of cytochrome $P\text{-}450_{scc}$. *Biochemistry* **28**, 6899–6907
5. Tuls, J., Geren, L., and Millett, F. (1989) Fluorescent isothiocyanate specifically modifies lysine 338 of cytochrome $P\text{-}450_{scc}$ and inhibits adrenodoxin binding. *J. Biol. Chem.* **264**, 16421–16425
6. Morohashi, K., Fujii-Kuriyama, Y., Okada, Y., Sogawa, K., Hirose, T., Inayama, S., and Omura, T. (1984) Molecular cloning and nucleotide sequence of cDNA for mRNA of mitochondrial cytochrome P-450(SCC) of bovine adrenal cortex. *Proc. Natl. Acad. Sci. USA* **81**, 4647–4651
7. Morohashi, K., Yoshioka, H., Gotoh, O., Okada, Y., Yamamoto, K., Miyata, T., Sogawa, K., Fujii-Kuriyama, Y., and Omura, T. (1987) Molecular cloning and nucleotide sequence of DNA of mitochondrial cytochrome P-450(11β) of bovine adrenal cortex. *J. Biochem.* **102**, 559–568

8. Usui, E., Noshiro, M., and Okuda, K. (1990) Molecular cloning of cDNA for vitamin D_3 25-hydroxylase from rat liver mitochondria. *FEBS Lett.* **262**, 135–138
9. Takeyama, K.-i., Kitanaka, S., Sato, T., Kobori, M., Yanagisawa, J., and Kato, S. (1997) 25-Hydroxyvitamin D_3 1α-hydroxylase and vitamin D synthesis. *Science* **277**, 1827–1829
10. Chen, K.-S., Prahl, J.M., and DeLuca, H.F. (1993) Isolation and expression of human 1,25-dihydroxyvitamin D_3 24-hydroxylase cDNA. *Proc. Natl. Acad. Sci. USA* **90**, 4543–4547
11. Wada, A. and Waterman, M.R. (1992) Identification by site-directed mutagenesis of two lysine residues in cholesterol side chain cleavage cytochrome P450 that are essential for adrenodoxin binding. *J. Biol. Chem.* **267**, 22877–22882
12. Pikuleva, I.A., Cao, C., and Waterman, M.R. (1999) An additional electrostatic interaction between adrenodoxin and P450c27 (CYP27A1) results in tighter binding than between adrenodoxin and P450scc (CYP11A1). *J. Biol. Chem.* **274**, 2045–2052
13. Tsubaki, M., Hiwatashi, A., and Ichikawa, Y. (1989) Conformational change of the heme moiety of ferrous cytochrome P-450_{scc}-phenyl isocyanide complex upon binding of reduced adrenodoxin. *Biochemistry* **28**, 9777–9784
14. Tsubaki, M., Hiwatashi, A., Fujimoto, Y., Ikekawa, N., Ichikawa, Y., and Hori, H. (1988) Electron paramagnetic resonance study of ferrous cytochrome P-450_{scc}-nitric oxide complexes: Effects of 20(*R*),22(*R*)-dihydroxycholesterol and reduced adrenodoxin. *Biochemistry* **27**, 4856–4862
15. Tsubaki, M., Yoshikawa, S., Ichikawa, Y., and Yu, N.-T. (1992) Effects of cholesterol side-chain groups and adrenodoxin binding on the vibrational modes of carbon monoxide bound to cytochrome P-450_{scc}: Implications of the productive and nonproductive substrate bindings. *Biochemistry* **31**, 8991–8999
16. Shimada, H., Nagano, S., Ariga, Y., Unno, M., Egawa, T., Hishiki, T., Ishimura, Y., Masuya, F., Obata, T., and Hori, H. (1999) Putidaredoxin-cytochrome P450cam interaction. Spin state of the heme iron modulates putidaredoxin structure. *J. Biol. Chem.* **274**, 9363–9369
17. Tsubaki, M., Tomita, S., Tsuneoka, Y., and Ichikawa, Y. (1986) Characterization of two cysteine residues in cytochrome P-450_{scc}: chemical identification of the heme-binding cysteine residue. *Biochim. Biophys. Acta* **870**, 564–574
18. Hiwatashi, A., Sakihama, N., Shin, M., and Ichikawa, Y. (1986) Heterogeneity of adrenocortical ferredoxin. *FEBS Lett.* **209**, 311–315
19. Tsubaki, M., Hiwatashi, A., Ichikawa, Y., and Hori, H. (1987) Electron paramagnetic resonance study of ferrous cytochrome P-450_{scc}-nitric oxide complexes: Effects of cholesterol and its analogues. *Biochemistry* **26**, 4527–4534
20. Imai, M., Shimada, H., Watanabe, Y., Matsushima-Hibiya, Y., Makino, R., Koga, H., Horiuchi, T., and Ishimura, Y. (1989) Uncoupling of the cytochrome P-450cam monooxygenase reaction by a single mutation, threonine-252 to alanine or valine: A possible role of the hydroxy amino acid in oxygen activation. *Proc. Natl. Acad. Sci. USA* **86**, 7823–7827
21. Tsubaki, M., Kobayashi, K., Ichise, T., Takeuchi, F., and Tagawa, S. (2000) Diethylpyrocarbonate-modification abolishes fast electron accepting ability of cytochrome b_{561} from ascorbate but does not influence on electron donation to monodehydroascorbate radical: Distinct roles of two heme centers for electron transfer across the chromaffin vesicle membranes. *Biochemistry* **39**, 3276–3284
22. Orme-Johnson, N.R., Light, D.R., White-Stevens, R.W., and Orme-Johnson, W.H. (1979) Steroid binding properties of beef adrenal cortical cytochrome P-450 which catalyzes the conversion of cholesterol into pregnenolone. *J. Biol. Chem.* **254**, 2103–2111
23. Lipscomb, J.D. (1980) Electron paramagnetic resonance detectable states of cytochrome P-450_{cam}. *Biochemistry* **19**, 3590–3599
24. Cupp, J.R. and Vickery, L.E. (1989) Adrenodoxin with a COOH-terminal deletion (des 116-128) exhibits enhanced activity. *J. Biol. Chem.* **264**, 1602–1607
25. Okamura, T., John, M.E., Zuber, M.X., Simpson, E.R., and Waterman, M.R. (1985) Molecular cloning and amino acid sequence of the precursor form of bovine adrenodoxin: Evidence for a previously unidentified COOH-terminal peptide. *Proc. Natl. Acad. Sci. USA* **82**, 5705–5709
26. Tsubaki, M., Hiwatashi, A., and Ichikawa, Y. (1986) Effects of cholesterol and adrenodoxin binding on the heme moiety of cytochrome P-450_{scc}: A resonance Raman study. *Biochemistry* **25**, 3563–3569
27. Hinz, M.J., Mock, D.M., Peterson, L.L., Tuttle, K., and Peterson, J.A. (1982) Equilibrium and kinetic studies of the interaction of cytochrome P-450_{cam} and putidaredoxin. *J. Biol. Chem.* **257**, 14324–14332
28. Koga, H., Sagara, Y., Yaoi, T., Tsujimura, M., Nakamura, K., Sekimizu, K., Makino, R., Shimada, H., Ishimura, Y., Yura, K., Go, M., Ikeguchi, M., and Horiuchi, T. (1993) Essential role of the Arg^{112} residue of cytochrome P450cam for electron transfer from reduced putidaredoxin. *FEBS Lett.* **331**, 109–113
29. Shiro, Y., Iizuka, T., Makino, R., Ishimura, Y., and Morishima, I. (1989) ^{15}N NMR study on cyanide ($C^{15}N^-$) complex of cytochrome P-450_{cam}. Effects of d-camphor and putidaredoxin on the iron-ligand structure. *J. Am. Chem. Soc.* **111**, 7707–7711
30. Makino, R., Iizuka, T., Ishimura, Y., Uno, T., Nishimura, Y., and Tsuboi, M. (1984) An anomalous Fe-CO stretching vibration for the CO complex of cytochrome P450cam in *Proceedings of the Ninth International Conference on Raman Spectroscopy*, pp. 492–493, The Chemical Society of Japan, Tokyo
31. Pochapsky, T.C., Ye, X.M., Ratnaswamy, G., and Lyons, T.A. (1994) An NMR-derived model for the solution structure of oxidized putidaredoxin, a 2-Fe, 2-S ferredoxin from *Pseudomonas*. *Biochemistry* **33**, 6424–6432
32. Pochapsky, T.C., Ratnaswamy, G., and Patera, A. (1994) Redox-dependent ^1H NMR spectral features and tertiary structural constraints on the C-terminal region of putidaredoxin. *Biochemistry* **33**, 6433–6441
33. Müller, A., Muller, J.J., Muller, Y.A., Uhlmann, H., Bernhardt, R., and Heinemann, U. (1998) New aspects of electron transfer revealed by the crystal structure of a truncated bovine adrenodoxin, Adx(4-108). *Structure* **6**, 269–280
34. Pikuleva, I.A., Tesh, K., Waterman, M.R., and Kim, Y. (2000) The tertiary structure of full-length bovine adrenodoxin suggests functional dimers. *Arch. Biochem. Biophys.* **373**, 44–55
35. Uhlmann, H., Kraft, R., and Bernhardt, R. (1994) C-terminal region of aderenodoxin affects its structural integrity and determines differences in its electron transfer function to cytochrome P-450. *J. Biol. Chem.* **269**, 22557–22564
36. Pochapsky, T.C., Lyons, T.A., Kazanis, S., Arakaki, T., and Ratnaswamy, G. (1996) A structure-based model for cytochrome P450cam-putidaredoxin interactions. *Biochimie* **78**, 723–733
37. Tsubaki, M. and Ichikawa, Y. (1985) Resonance Raman detection of a ν(Fe-CO) stretching frequency in cytochrome P-450_{scc} from bovine adrenocortical mitochondria. *Biochim. Biophys. Acta* **827**, 268–274
38. Tsai, R., Yu, C.A., Gunsalus, I.C., Peisach, J., Blumberg, W., Orme-Johnson, W.H., and Beinert, H. (1970) Spin-state changes in cytochrome P-450_{cam} on binding of specific substrates. *Proc. Natl. Acad. Sci. USA* **66**, 1157–1163
39. Unno, M., Christian, J.F., Benson, D.E., Gerber, N.C., Sligar, S.G., and Champion, P.M. (1997) Resonance Raman investigation of cytochrome P450_{cam} complexed with putidaredoxin. *J. Am. Chem. Soc.* **119**, 6614–6620
40. Lambeth, J.D., Seybert, D.W., Lancaster, J.R., Jr., Salerno, J.C., and Kamin, H. (1982) Steroidogenic electron transport in adrenal cortex mitochondria. *Mol. Cell. Biochem.* **45**, 13–31
41. Kido, T. and Kimura, T. (1979) The formation of binary and ternary complexes of cytochrome P-450_{scc} with adrenodoxin and adrenodoxin reductase-adrenodoxin complex. The implication in ACTH function. *J. Biol. Chem.* **254**, 11806–11815
42. Hara, T. and Takeshima, M. (1994) Conclusive evidence of a quaternary cluster model for cholesterol side chain cleavage reaction catalyzed by cytochrome P450scc in *Cytochrome P450*, 8th International Conference (Lechner, M.C., ed.) pp. 417–420, John Libbey Eurotext, Paris

43. Muller, J.J., Lapko, A., Bourenkov, G., Ruckpaul, K., and Heinemann, U. (2001) Adrenodoxin reductase-adrenodoxin complex structure suggests electron transfer path in steroid biosynthesis. *J. Biol. Chem.* **276**, 2786–2789
44. Müller, E.-C., Lapko, A., Otto, A., Müller, J.J., Ruckpaul, K., and Heinemann, U. (2001) Covalently crosslinked complexes of bovine adrenodoxin with adrenodoxin reductase and cytochrome P450scc. Mass spectrometry and Edman degradation of complexes of the steroidogenic hydroxylase system. *Eur. J. Biochem.* **268**, 1837–1843